DOI 10.24425/aee.2024.149928

Electric vehicle motor fault diagnosis using improved wavelet packet decomposition and particle swarm optimization algorithm

WENFANG ZHENG ✉, TIEYING WANG

Xinxiang Vocational and Technical College
Xinxiang 453000, China
e-mail: {✉ hnzwenfang/18537307963}@163.com

(Received: 10.24.2023, revised: 07.05.2024)

Abstract: This study addresses the issue of diagnosing faults in electric vehicle motors and presents a method utilizing Improved Wavelet Packet Decomposition (IWPD) combined with particle swarm optimization (PSO). Initially, the analysis focuses on common demagnetization faults, inter turn short circuit faults, and eccentricity faults of permanent magnet synchronous motors. The proposed approach involves the application of IWPD for extracting signal feature vectors, incorporating the energy spectrum scale, and extracting the feature vectors of the signal using the energy spectrum scale. Subsequently, a binary particle swarm optimization algorithm is employed to formulate strategies for updating particle velocity and position. Further optimization of the binary particle swarm algorithm using chaos theory and the simulated annealing algorithm results in the development of a motor fault diagnosis model based on the enhanced particle swarm optimization algorithm. The results demonstrate that the chaotic simulated annealing algorithm achieves the highest accuracy and recall rates, at 0.96 and 0.92, respectively. The model exhibits the highest fault accuracy rates on both the test and training sets, exceeding 98.2%, with a minimal loss function of 0.0035. Following extraction of fault signal feature vectors, the optimal fitness reaches 97.4%. In summary, the model constructed in this study demonstrates effective application in detecting faults in electric vehicle motors, holding significant implications for the advancement of the electric vehicle industry.

Key words: chaos theory, motor fault diagnosis, PSO, simulated annealing algorithm, wavelet packet decomposition

1. Introduction

In response to the escalating issue of environmental pollution, the emergence of new energy vehicles has become imperative. Electric vehicles, as prominent representatives of new energy vehicles, are increasingly scrutinized for their performance and safety. The motor, functioning as the driving component and power core of electric vehicles, significantly influences their overall performance and safety. Consequently, there is an urgent need to employ appropriate methods for timely and precise fault diagnosis [1].

The wavelet transform, a signal analysis method combining the localization concept of the short-time Fourier transform with adaptive frequency capabilities, has overcome the limitations of fixed window sizes and found extensive applications in fault diagnosis. However, during the decomposition process, only low-frequency signals are subjected to further decomposition, while high-frequency signals are not, resulting in a decrease in frequency resolution as frequencies rise. This limitation has led to the development of wavelet packet decomposition [2, 3].

Particle Swarm Optimization (PSO), an evolutionary computing technique, begins with random solutions and iteratively searches for the optimal solution, evaluating. solution quality via fitness. However, situations may arise where the cluster number is not an integer. To address this, Binary Particle Swarm Optimization (BPSO) is employed to formulate strategies for updating particle velocity and position, reducing both storage space and computational complexity [4, 5].

Against this backdrop, this study introduces a method for extracting fault signal feature vectors based on energy spectrum and constructs a Motor Fault Diagnosis (MFD) model using an improved PSO algorithm. Two primary innovations are highlighted in this research. First, the BPSO algorithm is improved by incorporating chaos theory and Simulated Annealing (SA) algorithms. Second, the study is organized into four parts. The first part involves an analysis of the current research status; The second part delves into the analysis of wavelet packet decomposition, proposing a fault signal feature vector extracting method utilizing energy spectrum. Additionally, it establishes the MFD model based on the chaos-SA-BPSO algorithm; The third part focuses on analyzing the application effects of the proposed model.

The concluding section provides a comprehensive summary of the entire research endeavor.

2. Related works

The motor, serving as the propulsive element of electric vehicles, undergoes fault diagnosis crucial for enhancing vehicle performance and safety. Addressing the susceptibility of traditional motor fault diagnosis methods to varying operational conditions, Long *et al*. introduced a vision-based motor fault diagnosis method. This approach aims to mitigate the impact of changing conditions, thereby enhancing feature extraction capabilities. The results indicate that this method, requiring minimal data training and learning, demonstrates feasibility and effectiveness [6].

Wang *et al*. highlighted the limitations of traditional cellular neural networks, wherein increasing layers lead to reduced feature resolution and information loss. Moreover, the fixed nuclear size makes traditional cellular neural networks unsuitable for MFD. To address this, they proposed a cascaded convolutional neural network with progressive optimization, specifically tailored for motor fault diagnosis [7].

In response to the computational challenges hindering the application of deep learning models in fault diagnosis, Wang *et al*. introduced a lightweight multisensory fusion model. This model, designed for induction motor data fusion and diagnosis, outperforms other neural networks by accurately predicting fault modes in a shorter time frame [8].

Considering limitation of existing diagnostic models based on convolutional neural networks, which assume stable motor operation conditions, Xu *et al*. proposed a lightweight multi-scale convolutional neural network model for motor fault identification under non-stationary conditions, aiming to advance Motor Fault Diagnosis (MFD) technology. Experimental outcomes indicate significant improvements under various non-stationary conditions [9].

For induction MFD, Fu P. *et al*. introduced a multi-mode neural network based on dynamic routing with a multi-mode deep learning framework. They designed a multi-mode feature extraction scheme using multi-source information for dimensionality reduction and invariant feature capture. The experiment outcomes demonstrate that the proposed method's strong performance, effectiveness, and stability [10].

Addressing the manpower-intensive nature of traditional sensor-based fault detection methods, Chikkam *et al*. proposed a methodology for estimating the faults in each component of the induction motor by analyzing motor current characteristics. Additionally, they suggested estimating fault severity using discrete wavelet transform coefficients based on feature extraction. Experimental results affirm the proposed method's accuracy and feasibility [11].

Wavelet packet decomposition utilizes analysis tree for presenting the wavelet packet, employing multiple iterations of wavelet transformation for a details analysis of the input signal. This approach offers a more refined analytical method for signal processing. Singla *et al*. addressed the intermittent and random nature of solar photovoltaic output, posing a threat to power safety and reliability in solar grid-connections. They introduced a hybrid model incorporating full wavelet packet decomposition and bidirectional long short-term memory. The model accurately estimates solar irradiance, demonstrating feasibility and effectiveness [12].

In the context of early fault detection and type recognition in rolling bearings, Lu *et al*. integrated wavelet packet decomposition with graph theory to extract the correlation information among wavelet packet coefficients. They proposed a two-stage framework for early warning detection and fault recognition, capable of identifying both the time and position of early faults, as well as the fault type. Experimental results indicate the framework's effectiveness and superiority [13].

Addressing the challenge of bearing fault prediction, Habbouche *et al*. introduced a novel data-driven method for bearing prediction. This method, based on wavelet packet decomposition f bidirectional long short-term memory (BLSTM), is employed for preprocessing and tracking the degradation processes, ultimately estimating the remaining service life of the bearings. The results indicate the effectiveness of the proposed approach in detecting the degradation processes of bearings and accurately predicting their remaining service life [14].

Liu *et al*. addressed the recognition challenges associated with coal-rock interfaces by proposing a recognition system based on wavelet packet decomposition and fuzzy neural networks. Employing various sensors to gather response signals from the shearer, the system achieved the extraction of multi-signal features and data fusion for coal-rock interface recognition. The results demonstrate that the proposed system exhibits high recognition accuracy and holds practical feasibility [15].

Sairamya *et al*. addressed the limited application of wavelet transform in classifying types of epileptic seizures from normal electroencephalogram (EEG) signals. They employed both discrete

wavelet transforms and wavelet packet decomposition to automatically diagnose epileptic seizures and categorize their types. The results indicated that discrete wavelet transform achieved a higher classification accuracy [16].

In view of the time-consuming and error-prone problem of visual detection and interpretation of seizure types, Tang *et al*. proposed an innovative classification method that integrates wavelet packet decomposition and local de-trend wave analysis into a computer-aided diagnostic systems. This method aims to automatically and accurately classify various seizure types. The results indicate that the proposed approach achieves a high overall classification accuracy, demonstrating certain advantages [17].

To sum up, despite the extensive research conducted by previous scholars on MFD, a majority of the diagnostic methods have relied heavily on neural networks, presenting challenges related to acquiring training samples and extended training times. Consequently, the study of electric vehicle motor fault diagnosis using the enhanced wavelet packet decomposition (WPD) and particle swarm optimization (PSO) algorithm holds significant practical application value and promising prospects.

3. MFD using IWPD and PSO

Ensuring optimal performance and safety in electric vehicles necessitates meticulous motor fault detection. Motors exhibit various fault types, contributing to the complexity of fault diagnosis. To address this challenge, the study employs WPD for data preprocessing. Subsequently, it extracts fault signal feature vector based on energy spectrum. The traditional PSO algorithm is then improved, leading to the construction of an MFD model utilizing the CSA–BPSO algorithm.

3.1. WPD and feature vector extracting

The robust development of the electric vehicle industry stands as a pivotal measure for effectively mitigating greenhouse gas emissions and diminishing reliance on oil-dependent transportation [18]. Given the challenging factors of harsh driving environments and complex driving conditions, the likelihood of failures in electric vehicles is notably high. The drive motor, comprising the motor controller, drive motor, and reducer, serves as the power core of electric vehicles. Motor failures are categorized based on severity into four types: slight fault, general fault, serious fault and fatal fault [19].

Model-based fault diagnosis primarily relies on a fundamental wave mathematical model established according to the operating principle and characteristics of the motor. This model is then compared with the detected operating data of the motor and the calculated values derived from the model. The fault diagnosis process is illustrated in Fig. 1.

Permanent magnet synchronous motors, relying on permanent magnets for excitation, boast high efficiency and power density, making them extensively utilized in electric vehicles. Common faults of permanent magnet synchronous motor include loss of magnetic fault, inter-turn short circuit fault and eccentric fault. The loss of magnetic flux fault is unique to permanent magnet synchronous motors and occurs when the permanent magnet undergoes prolonged operation, experiencing demagnetization due to the combined interference of electrical and environmental factors. This demagnetization compromises the magnetic induction performance of the permanent

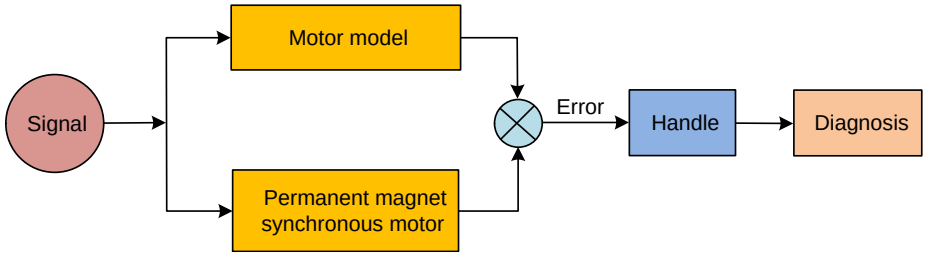

Fig. 1. Fault diagnosis

magnet [20]. Simultaneously, low-frequency components emerge around the fundamental frequency of the current signal, resulting in characteristic frequencies as illustrated in Eq. (1).

$$f_{dmg} = f_s \left| 1 \pm \frac{k}{p} \right|, \tag{1}$$

where: f_s represents the power frequency of the motor, p provides an overview of the number of pole pairs of the magnetic poles.

The inter-turn short-circuit fault will cause the current in the motor winding to produce imbalance, damage the electrical performance, the most obvious feature is manifested in the rotor current will produce more current harmonic components, the existence of this phenomenon will cause the generation of non-power frequency, as illustrated in Eq. (2).

$$f_{sc} = f_s \left(v \frac{Z}{P} \pm 1 \right), \tag{2}$$

where: v is a positive integer, Z is the number of stator slots in the motor.

By analyzing the collected electrical parameters, the characteristic signal of the fault can be learned. Eccentric fault will lead to unbalanced distribution of air gap in the motor, and then cause the imbalance of magnetic flux in the air gap, at the same time, there will be fault harmonic components in the three-phase line current, so it can be realized by means of the amplitude of the current spectrum of side band components to identify and judge the eccentric fault. The specific frequency calculation of the sideband component is illustrated in Eq. (3).

$$f_{px} = f_s \left[1 \pm \left(\frac{2k - 1}{p} \right) \right]. \tag{3}$$

The Permanent Magnet Synchronous Motor (PMSM) primarily consists of components such as the stator, rotor, and end cover, as illustrated in Fig. 2. The structure is relatively straightforward, and its configuration alongside the drive system is depicted in Fig. 2.

Wavelet transform, a time-frequency signal analysis method in the field of fault diagnosis, finds extensive application in the analysis of non-stationary signals. Wavelet transform is often used to process, and the low-frequency part of the signal is decomposed to determine the wavelet threshold, and then the signal is reconstructed to achieve the purpose of noise reduction. The

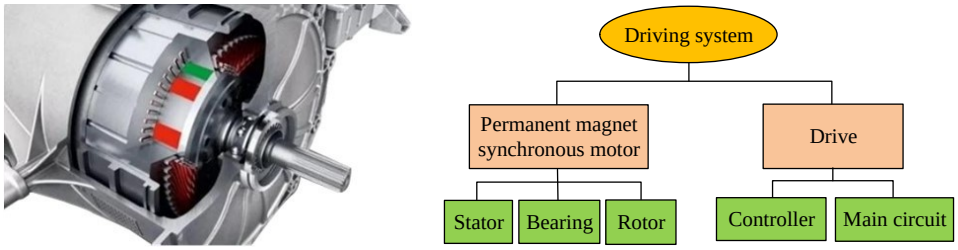

(a) Structure of the drive motor (b) Drive system structure

Fig. 2. Structure and drive system of permanent magnet synchronous motor

wavelet packet transform is illustrated in Eq. (4).

$$\begin{cases} \mu_{2n}(t) = \sqrt{2}\sum_{k=0}^{2N-1} h_k \mu_n(2t-k) \\ \mu_{2n+1}(t) = \sqrt{2}\sum_{k=0}^{2N-1} g_k \mu_n(2t-k) \end{cases}, \tag{4}$$

where: k and n are the translation variables, $\mu_n(t)$ is the original signal sequence, g_k is a high-pass filter, h_k is a low-pass filter.

Wavelet packet decomposition is the optimization method of wavelet transform, determine the number of decomposition layers, treat the non-stationary signal multi-level frequency band division, and the signal low frequency and high frequency part of the layer-by-layer decomposition, can effectively reduce interference, improve the signal-to-noise ratio role. The wavelet packet decomposition is illustrated in Eq. (5).

$$\begin{cases} \phi_k^{i,2m} = \sum_{n\in Z} h_{n-2k}\phi_n^{i-1,m} \\ \phi_k^{i,2m+1} = \sum_{n\in Z} g_{n-2k}\phi_n^{i-1,m} \end{cases}, \tag{5}$$

where: i is the scale variable, m is the frequency variable, $\phi_k^{i,2m}$ and $\phi_k^{i,2m+1}$ are the wavelet coefficients, h_{n-2k} is the low-pass filter, g_{n-2k} is the high-pass filter.

The application of wavelets in signal processing requires careful consideration of both signal processing needs and computational efficiency, encompassing four primary steps. The first step is to determine the number of layers of WPD according to the signal demand. The second step is to select the wavelet packet base function and optimal tree according to the entropy standard. The third step, according to the demand and the characteristics of the signal, determine the appropriate threshold to quantize the wavelet packet decomposition coefficient. In the fourth step, the quantization coefficient is used to reconstruct the wavelet packet. When the electric vehicle drive motor fails, the characteristics of the differential energy signal can be retained for energy detection. The original signal of the wavelet transform is studied in the square integrable real number space, and

the wavelet norm is obtained, as illustrated in Eq. (6).

$$\|f\|_2^2 = \int_R |f(x)|^2 \, \mathrm{d}x. \tag{6}$$

If the studied signal sequence has wavelet, the wavelet transform and the original signal have the characteristics of equal energy, and there is an equality relationship as illustrated in Eq. (7).

$$\int_R \mathrm{d}a \int_R \mathrm{d}b \left| \frac{Wf(a,b)}{a} \right|^2 = \|f\|_2^2 \left(\forall f \in L^2(R) \right). \tag{7}$$

The introduction of electric vehicles into the market aims to reduce reliance on internal combustion engine-driven transportation systems, yet this transition paradoxically increases the burden on the current power grid [21, 22]. The determination of feature vectors is helpful for fault detection, can use the actual working conditions of the drive motor to determine the feature vector, the general use of the feature signals is the working torque of the drive motor, current, vibration, voltage and working temperature, etc. For example, distributed generators can detect possible faults by monitoring the vibration of the generator [23, 24].

However, direct analysis of these signals results in significant data fluctuations, rendering fault diagnosis challenging and introducing substantial errors. Using wavelet packet decomposition to decompose and extract the signal feature vector can shorten the training time and improve the probability of MFD. The structure of WPD is depicted in Fig. 3.

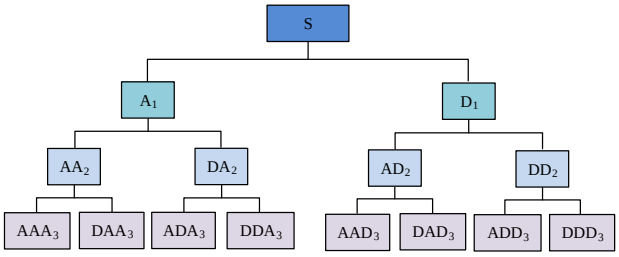

Fig. 3. The WPD structure

According to the wavelet packet energy spectrum, it becomes possible to acquire the energy distribution and inherent characteristics of the original signal. For expressing the energy of the signal directly, the energy spectrum scale diagram is used to analyze the signal when the motor fails. The energy spectrum scale is utilized for extracting the feature vector of the signal, and the method is to analyze the existing differences, as illustrated in Eq. (8).

$$\begin{cases} E = \sqrt{\left(\sum_{i=0}^{7} |E_{3i}|^2 \right)} \\ Sk = \dfrac{E_{3i}}{E} \\ T = \left[\dfrac{E_K^0}{E}, \dfrac{E_K^1}{E}, \ldots, \dfrac{E_K^7}{E} \right] \end{cases}, \tag{8}$$

where: E is the total energy of the signal, T is the feature vector after energy spectrum normalization.

Using wavelet packet decomposition to process signals, time domain feature parameters are selected as feature vectors. The commonly selected time domain feature parameters include signal peak, effective mean and kurtosis index, etc. The index is calculated as illustrated in Eq. (9).

$$\begin{cases} x_m = \max(|x_i|) \\ X_{\text{rms}} = \dfrac{1}{N}\sqrt{\displaystyle\sum_{i=1}^{N} x_i^2(t)} \\ K_4 = \dfrac{\dfrac{1}{N}\displaystyle\sum_{i=1}^{N} x_i^4(t)}{X_{\text{rms}}^4} \end{cases}, \tag{9}$$

where: x_m is the signal peak, X_{rms} is the effective mean, N is the data length, K_4 is the kurtosis index.

3.2. Construction of the MFD based on CSA–BPSO algorithm

The PSO algorithm, an intelligent optimization technique inspired by the predatory behavior of bird flocks, exhibits certain similarities with the optimization process of models when analyzing bird foraging behavior. Particularly effective in handling complex optimization problems, the PSO algorithm conducts a global search, significantly enhancing optimization efficiency and precision. Firstly, determine a D-dimensional space, treat each bird as a particle, and input the particle's position information into the fitness function. The smaller the value obtained, the better the particle's spatial position. By iterating, the position of particles can be updated, and once all iteration operations are completed, the optimal solution can be output. The velocity and position updates of particle i are illustrated in Eq. (10).

$$\begin{cases} V_{ij(t+1)} = \omega V_{ij(t)} + c_1 r_1 \left(p\text{best}_{ij(t)} - x_{ij(t)}\right) + c_2 r_2 \left(g\text{best}_{ij(t)} - x_{ij(t)}\right) \\ x_{ij(t+1)} = x_{ij(t)} + v_{ij(t+1)} \end{cases}, \tag{10}$$

where: ω is the inertia factor, c_1 and c_2 represent the learning factor, whose values directly interfere with the convergence of the particle. $v_{ij(t)}$ and $v_{ij(t+1)}$ are the components of the particle's velocity in the j dimension when it evolves to the t and $t+1$ generations, $p\text{best}_{ij(t)}$ is the component of the individual's optimal position in the j dimension when it evolves to the t generation, $x_{ij(t)}$ and $x_{ij(t+1)}$ are the components of the individual's optimal position in the j dimension when it evolves to the t and $t+1$ generation, $g\text{best}_{ij(t)}$ is the component of the entire particle swarm's optimal position in the j dimension when it evolves to the t generation.

The specific process of the PSO algorithm is depicted in Fig. 4.

In traditional PSO algorithms, the factors c and r can result in non-integer cluster numbering. To address this issue, this study employs the Binary Particle Swarm Optimization (BPSO) algorithm to formulate strategies for updating particle velocity and position. The BPSO algorithm is an algorithm proposed on the basis of the PSO algorithm to solve discrete problems in space. It can handle discrete space search and discrete model solving problems. After the PSO algorithm

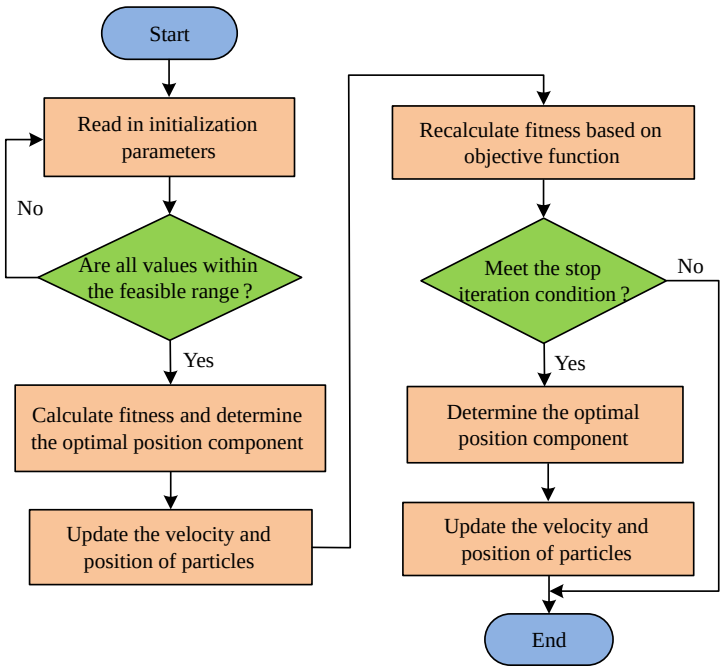

Fig. 4. PSO flowchart

updates the particle velocity, the velocity is expressed as a probability value, and the probability of taking position x_{id} as 1 is illustrated in Eq. (11).

$$S(v_{id}) = \frac{1}{1 + e^{-v_{id}}}, \tag{11}$$

where v_{id} is the particle velocity.

After obtaining the probability value of velocity, the determination of particle position value is illustrated in Eq. (12).

$$x_{id} = \begin{cases} 1, & \text{if rand}() \le S(v_{id}) \\ 0, & \text{otherwise} \end{cases}, \tag{12}$$

where rand() is a random number with a value of [0–1].

Nevertheless, the BPSO algorithm also suffers from premature convergence and is prone to local convergence. Therefore, this study proposes the Chaos Simulated Annealing (CSA) algorithm to improve the BPSO algorithm. Chaos, a phenomenon confined to nonlinear deterministic systems within limited spaces, exhibits complex and irregular motion, ergodicity, inherent randomness, and regularity. Research using the ergodicity of chaos theory to rearrange the positions of particles and enhance the global search performance of the algorithm. Chaos is a logistic map, and the expression is illustrated in Eq. (13).

$$f(x) = \mu x(1 - x), \tag{13}$$

where μ is an adjustable parameter with a value in the range of [0, 4].

The SA algorithm is a heuristic, random search method for finding the optimal solution. It draws inspiration from the similarity between the annealing problem of crystalline substances in physics and the broader combinatorial optimization problem. The application process is not affected by the initial value size, and can solve nonlinear, discontinuous, and random objective function problems. It can obtain the optimal solution globally. The process of the simulated annealing algorithm is depicted in Fig. 5.

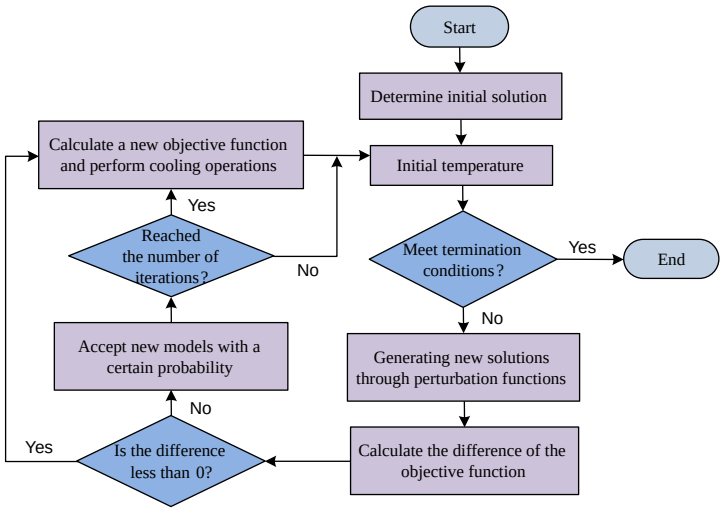

Fig. 5. Flow chart of simulated annealing algorithm

However, in practical applications, finding the optimal solution can be time-consuming, and using parameters for specific problem-solving can be challenging, often leading to simulated annealing failure. Therefore, this study utilizes the approximate random search characteristics of chaos to optimize the speed of searching for the optimal solution, and utilizes the ergodicity of chaos to avoid simulated annealing failure. It can traverse all states in the space without repetition within a certain search range, improving the effectiveness of solving the search.

The CSA algorithm builds upon the traditional SA algorithm by incorporating chaotic optimization to determine the initial value. It is assumed that N feasible solutions are searched for during the first iteration process, and the objective function values of N points are obtained through the solving process. Compare all the obtained objective function values to find the maximum and minimum value. The initial temperature value of the SA algorithm is illustrated in Eq. (14).

$$\begin{cases} T_0 = \dfrac{(\max f_k - \min f_k)}{\ln P_{r0}} \\ P_{r0} = \exp \dfrac{-\Delta C}{T_0} \end{cases}, \tag{14}$$

where: $\max f_k$ and $\min f_k$ are the maximum and min values, P_{r0} is the probability of accepting the new model, ΔC is the difference between the maximum and minimum values.

The structure of the MFD model based on WPD and CSA–BPSO algorithm is depicted in Fig. 6.

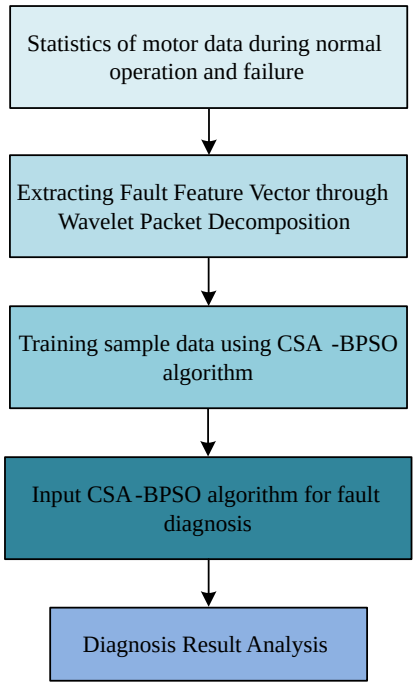

Fig. 6. Structure diagram of MFD model based on WPD and CSA–BPSO

4. Analysis of the effectiveness of MFD method based on IWPD and PSO algorithm

In order to diagnose faults in electric vehicle motors, a method for extracting fault signal feature vectors based on energy spectrum was proposed, and an MFD model based on the CSA–BPSO algorithm was established. However, its effectiveness requires further validation. The study primarily conducts analysis from two perspectives. First, it evaluates the effectiveness of the proposed feature extraction method and the improved algorithm. Subsequently, the effectiveness of the MFD model based on wavelet packet decomposition and the CSA–BPSO algorithm is assessed.

4.1. Effectiveness analysis of feature extraction methods and CSA–BPSO algorithm

To obtain the wavelet packet coefficients of each node and achieve signal reconstruction, the original signal was decomposed using WPD. The three-layer WPD of the obtained signal is depicted in Fig. 7.

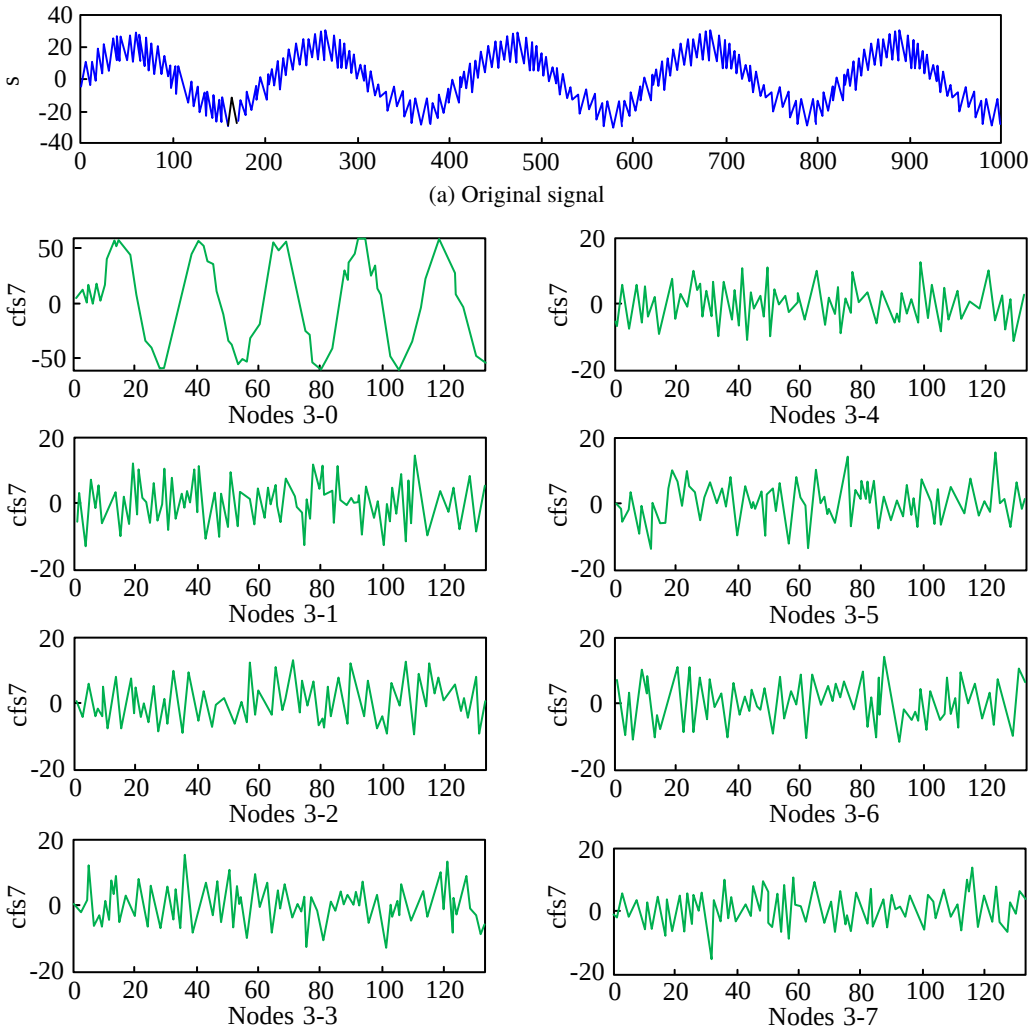

(a) Original signal

(b) Three-layer WPD

Fig. 7. Three layer WPD of signals

For verifying the feasibility of the proposed method for extracting fault signal feature vectors based on the energy spectrum, this study conducted a comparative analysis between the energy spectrum scale maps of vibration signals from a normally operating motor and a motor experiencing bearing faults. The experiment outcomes are given in Fig. 8. There are significant differences in the energy ratio of the same frequency band under different states, so it is feasible to use the energy spectrum scale for extracting the signal feature vectors.

To assess the performance of the proposed CSA algorithm, the research configured a population size of 100, an initial temperature of 100°, and a termination temperature of 10°C. The results were compared with SA algorithm and PSO algorithm, as shown in Fig. 9. As the number of

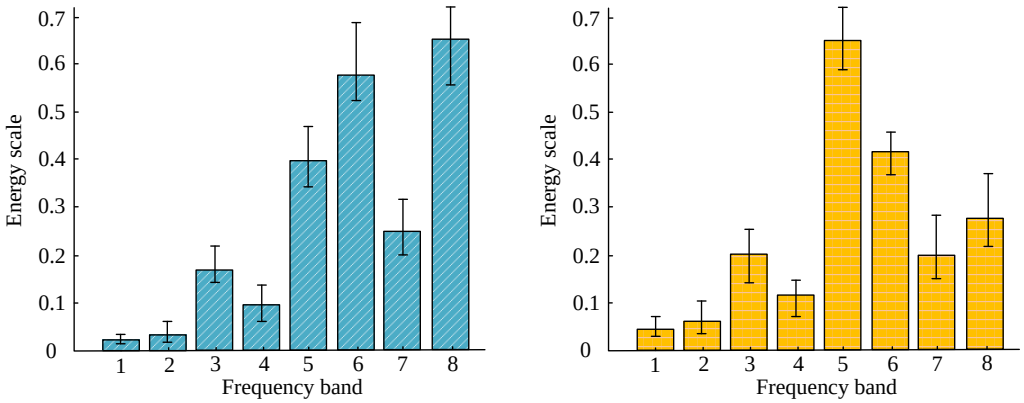

(a) Energy scale of vibration signals for normal operation

(b) Energy scale of vibration signal during bearing failure

Fig. 8. Energy spectrum scale maps under different states

iterations increases, the accuracy and recall of the three algorithms gradually increase. However, among the three algorithms, the CSA algorithm has the highest accuracy and recall rates, with 0.96 and 0.92 respectively, followed by the PSO algorithm, and the SA algorithm has the worst performance. These outcomes suggest that the chaos theory's quasi-random search properties contribute significantly to enhancing the performance of the SA algorithm, demonstrating a degree of feasibility and effectiveness.

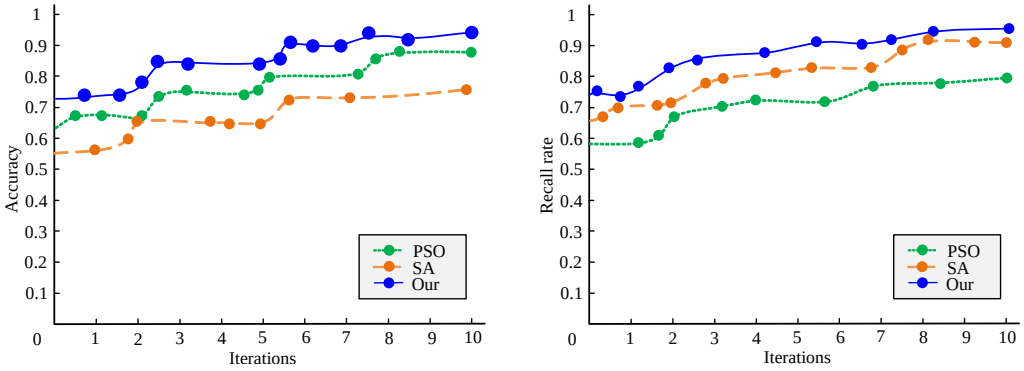

(a) Accuracy comparison results

(b) Recall rate comparison results

Fig. 9. Comparison results of accuracy and recall of three algorithms

To evaluate the performance of the CSA–BPSO algorithm, the study selected the Vehicle, Snow, and Wine datasets for testing. The maximum number of features was 60, the max categories number was 15, the population was set to 20, and the maximum number of iterations was set to 1 000. The results were compared with the BPSO algorithm and the SA-BPSO algorithm, as shown in Fig. 10. Among the three algorithms, the curve of CSA–BPSO algorithm exhibits an

increasing trend, showcasing superior global optimization ability. Both the BPSO algorithm and the SA-BPSO algorithm are prone to falling into local optima. Especially in the Wine dataset, the BPSO algorithm and SA-BPSO algorithm stopped searching when the number of iterations was between 200 and 250, while the CSA–BPSO algorithm also experienced a sudden increase when the number of iterations was around 620. These results indicate that the CSA–BPSO algorithm demonstrates robust global optimization performance.

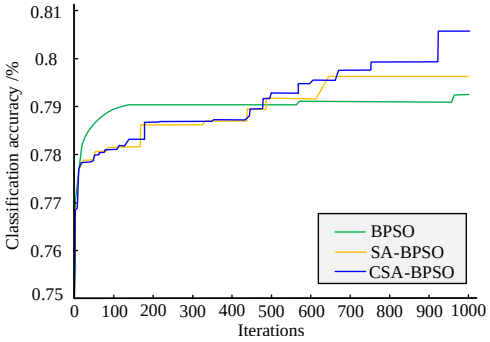

(a) Vehicle number aggregation

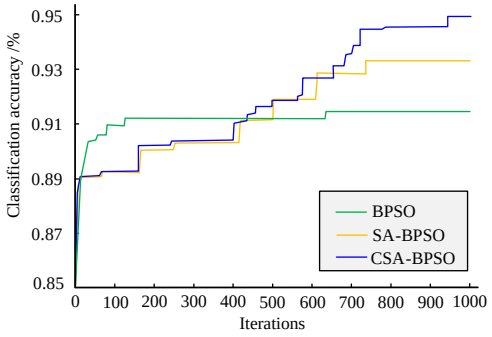

(b) Snow number aggregation

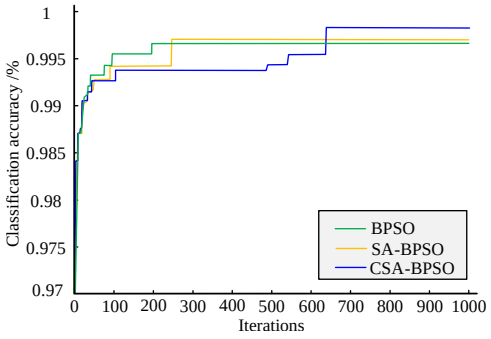

(c) Wine number aggregation

Fig. 10. Comparison of classification accuracy of three algorithms

4.2. Analysis of the effectiveness of the MFD model based on WPD and CSA–BPSO algorithm

For verifying the effectiveness of the MFD model based on wavelet packet decomposition and CSA–BPSO algorithm, this study employed an NI data acquisition card to capture current, voltage, and vibration signals from the drive motor. The collected data was then transmitted to the fault diagnosis model for comprehensive evaluation and analysis in the context of motor fault diagnosis. The parameters of the tested motor are detailed in Table 1.

The fault detection accuracy of the proposed model during both training and testing phases is depicted in Fig. 11. The proposed model has the highest fault detection accuracy on both the test and training sets, reaching over 98.2%, and has a small loss function of 0.0035. These findings

Table 1. Test the parameters of the motor

Electrical parameter items	**Parameter**
Rated torque	0.18 Nm
No-load speed	4 800 RPM
Rated speed	3 000 RPM
Number of pole pairs	2
Rated current	3.3 A
Rated voltage	24 VDC
No-load current	0.3 A
Rated power	60 W

signify that the MFD model, founded on wavelet packet decomposition and the CSA–BPSO algorithm, is applicable for detecting motor faults in electric vehicles. The model demonstrates a certain level of feasibility and effectiveness.

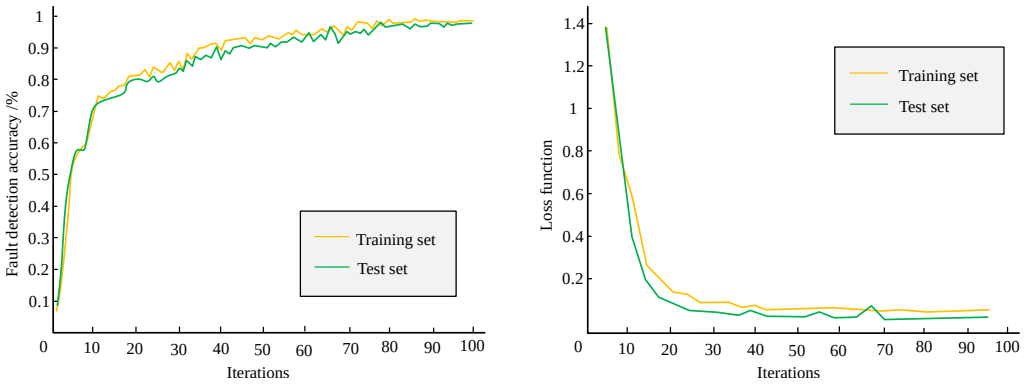

(a) Fault detection accuracy (b) Loss function

Fig. 11. Fault detection accuracy results

For verifying the effectiveness of the fault signal feature vector extraction method based on the energy spectrum, this study compared the MFD model based on wavelet packet decomposition and the CSA–BPSO algorithm with the MFD model based solely on the CSA–BPSO algorithm, as depicted in Fig. 12. The results illustrate a notable increase in fitness after the extraction of fault signal feature vectors, with the optimum fitness reaching 97.4%. This outcome suggests that the extraction of fault feature vectors comprehensively portrays the motor fault status, thereby enhancing diagnostic accuracy.

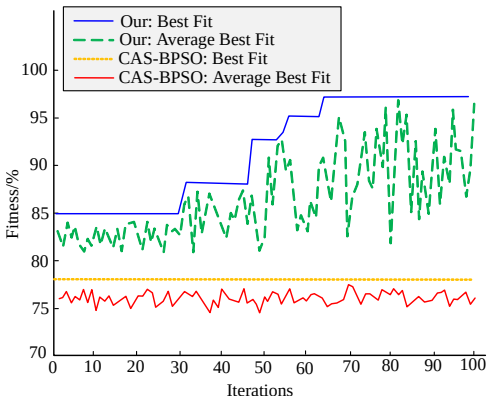

Fig. 12. Comparison results of fitness curves

5. Conclusion

In tandem with technological advancements and the escalating concerns surrounding environmental pollution, electric vehicles are gaining widespread acceptance in the market. In addressing the challenge of motor fault detection in electric vehicles, this study scrutinizes wavelet packet decomposition, proposing a method for extracting feature vectors from fault signals based on energy spectra. Additionally, an MFD model is established using the CSA–BPSO algorithm.

The findings reveal significant disparities in the energy ratio of the same frequency band under varying states, affirming the feasibility of employing the energy spectrum scale for feature vector extraction. Notably, the CSA algorithm demonstrates the highest accuracy and recall rates at 0.96 and 0.92, respectively, while the SA algorithm performs the worst. The beneficial impact of chaos theory's approximate random search characteristics on enhancing the SA algorithm's performance is evident.

In the Wine dataset, both the BPSO algorithm and the SA-BPSO algorithm cease searching between 200 and 250 iterations, while the CSA–BPSO algorithm experiences a sudden increase around 620th iteration. The proposed model attains the highest fault detection accuracy on both the test and training sets, surpassing 98.2%, accompanied by a minimal loss function of 0.0035. Following the extraction of fault signal feature vectors, a notable increase in fitness is observed, with the optimal fitness reaching 97.4%. This underscores the comprehensive representation of motor fault status achieved through the extraction of fault feature vectors.

In summary, the model devised in this study exhibits a degree of feasibility and effectiveness. However, it is essential to note that the study exclusively analyzed single faults such as inter-turn short circuits, demagnetization faults, and eccentricity faults in the motor. The absence of consideration for scenarios involving multiple faults may impact the practical application efficacy of the model, fail to meet the comprehensive fault diagnosis requirements of complex systems, and make it difficult to accurately identify composite faults. Consequently, future research should introduce more types of faults and perform fusion analysis on fault signals to develop a more robust motor multiple fault detection model.

References

[1] Jacobs B.W., Singhal V.R., *Shareholder value effects of the Volkswagen emissions scandal on the automotive ecosystem*, Production and Operations Management, vol. 29, no. 10, pp. 2230–2251 (2020), DOI: 10.1111/poms.13228.

[2] Othman G., Zeebaree D.Q., *The applications of discrete wavelet transform in image processing: A review*, Journal of Soft Computing and Data Mining, vol. 1, no. 2, pp. 31–43 (2020), DOI: 10.30880/jscdm.2020.01.02.004.

[3] Rinoshika A., Rinoshika H., *Application of multi-dimensional wavelet transform to fluid mechanics*, Theoretical and Applied Mechanics Letters, vol. 10, no. 2, pp. 98–115 (2020), DOI: 10.1016/j.taml.2020.01.017.

[4] Zeng N., Wang Z., Liu W., Zhang H., Hone K., Liu X., *A dynamic neighborhood-based switching particle swarm optimization algorithm*, IEEE Transactions on Cybernetics, vol. 52, no. 9, pp. 9290–9301 (2020), DOI: 10.1109/TCYB.2020.3029748.

[5] Lee J., Lee H., Nah W., *Minimizing the number of X/Y capacitors in an autonomous emergency brake system using the BPSO algorithm*, IEEE Transactions on Power Electronics, vol. 37, no. 2, pp. 1630–1640 (2021), DOI: 10.1109/TPEL.2021.3104671.

[6] Long Z., Zhang X., He M., Huang S., Qin G., Song D., Tang Y., Wu G., Liang W., Shao H., *Motor fault diagnosis based on scale invariant image features*, IEEE Transactions on Industrial Informatics, vol. 18, no. 3, pp. 1605–1617 (2021), DOI: 10.1109/TII.2021.3084615.

[7] Wang F., Liu R., Hu Q., Chen X., *Cascade convolutional neural network with progressive optimization for motor fault diagnosis under nonstationary conditions*, IEEE Transactions on Industrial Informatics, vol. 17, no. 4, pp. 2511–2521 (2020), DOI: 10.1109/TII.2020.3003353.

[8] Wang J., Fu P., Ji S., Li Y., Gao R.X., *A light weight multisensory fusion model for induction motor fault diagnosis*, IEEE/ASME Transactions on Mechatronics, vol. 27, no. 6, pp. 4932–4941 (2022), DOI: 10.1109/TMECH.2022.3169143.

[9] Xu Y., Yan X., Sun B., Liu Z., *Deep coupled visual perceptual networks for motor fault diagnosis under nonstationary conditions*, IEEE/ASME Transactions on Mechatronics, vol. 27, no. 6, pp. 4840–4850 (2022), DOI: 10.1109/TMECH.2022.3166839.

[10] Fu P., Wang J., Zhang X., Zhang L., Gao R.X., *Dynamic routing-based multimodal neural network for multi-sensory fault diagnosis of induction motor*, Journal of Manufacturing Systems, vol. 55, no. 4, pp. 264–272 (2020), DOI: 10.1016/j.jmsy.2020.04.009.

[11] Chikkam S., Singh S., *Condition monitoring and fault diagnosis of induction motor using DWT and ANN*, Arabian Journal for Science and Engineering, vol. 48, no. 5, pp. 6237–6252 (2023), DOI: 10.1109/ICEES51510.2021.9383729.

[12] Singla P., Duhan M., Saroha S., *A hybrid solar irradiance forecasting using full wavelet packet decomposition and bi-directional long short-term memory (BiLSTM)*, Arabian Journal for Science and Engineering, vol. 47, no. 11, pp. 14185–14211 (2022), DOI: 10.1007/s13369-022-06655-2.

[13] Lu G., Wen X., He G., Yi X., Yan P., *Early fault warning and identification in condition monitoring of bearing via wavelet packet decomposition coupled with graph*, IEEE/ASME Transactions on Mechatronics, vol. 27, no. 5, pp. 3155–3164 (2021), DOI: 10.1109/TMECH.2021.3110988.

[14] Habbouche H., Benkedjouh T., Zerhouni N., *Intelligent prognostics of bearings based on bidirectional long short-term memory and wavelet packet decomposition*, The International Journal of Advanced Manufacturing Technology, vol. 114, no. 1, pp. 145–157 (2021), DOI: 10.1007/s00170-021-06814-z.

[15] Liu Y., Dhakal S., Hao B., *Coal and rock interface identification based on wavelet packet decomposition and fuzzy neural network*, Journal of Intelligent and Fuzzy Systems, vol. 38, no. 4, pp. 3949–3959 (2020), DOI: 10.3233/jifs-179620.

[16] Sairamya N.J., Premkumar M.J., George S.T., Subathra M.S.P., *Performance evaluation of discrete wavelet transform, and wavelet packet decomposition for automated focal and generalized epileptic seizure detection*, IETE Journal of Research, vol. 67, no. 6, pp. 778–798 (2021), DOI: 10.1080/03772063.2019.1568206

[17] Tang L., Zhao M., Wu X., *Accurate classification of epilepsy seizure types using wavelet packet decomposition and local detrended fluctuation analysis*, Electronics Letters, vol. 56, no. 17, pp. 861–863 (2020), DOI: 10.1049/el.2020.1471.

[18] Yadav S., Sudman M.S.I., Dubey P.K., Srinivas R.V., Srisainath R., Devi V.C., *Development of an GA-RBF based Model for Penetration of Electric Vehicles and its Projections*, 2023 International Conference on Self Sustainable Artificial Intelligence Systems (ICSSAS), IEEE, pp. 1–6 (2023), DOI: 10.1109/ICSSAS57918.2023.10331883.

[19] Yang M., *Research on vehicle automatic driving target perception technology based on improved MSRPN algorithm*, Journal of Computational and Cognitive Engineering, vol. 1, no. 3, pp. 147–151 (2022), DOI: 10.47852/bonviewJCCE20514.

[20] Jiang S., Zhou B., Huang X., Xiong L., Wei J., *Fault-tolerant system design for doubly salient electromagnetic machine under loss of excitation*, IEEE Transactions on Power Electronics, vol. 37, no. 4, pp. 4589–4599 (2021), DOI: 10.1109/TPEL.2021.3123292.

[21] Dubey P.K., Singh B., Kumar V., Singh D., *A novel approach for comparative analysis of distributed generations and electric vehicles in distribution systems*, Electr. Eng., pp. 1–20 (2023), DOI: 10.1007/s00202-023-02072-2.

[22] Singh B., Dubey P.K., Singh S.N., *Recent optimization techniques for coordinated control of electric vehicles in super smart power grids network: A state of the art*, 2022 IEEE 9th Uttar Pradesh Section International Conference on Electrical, Electronics and Computer Engineering (UPCON), IEEE, pp. 1–7 (2022), DOI: 10.1109/UPCON56432.2022.9986471.

[23] Dubey P.K., Singh B., Patel D.K., Singh D., *Distributed generation current scenario in the world*, Int. J. Multidiscip. Res., vol. 5, no. 4, pp. 1–25 (2023), DOI: 10.36948/ijfmr.2023.v05i04.4625.

[24] Singh B., Dubey P.K., *Distributed power generation planning for DN using electric vehicles: Systematic attention to challenges and opportunities*, J. Ener. Stor., vol. 48, no. 1, pp. 1–42 (2022), DOI: 10.1016/j.est.2022.104030.